Colloid Polym Sci 277:513–518 (1999)

ORIGINAL CONTRIBUTION

M. Bonnet
K.-D. Rogausch
J. Petermann

The endothermic "annealing peak" of poly(phenylene sulphide) and poly(ethylene terephthalate)

Received: 27 October 1998
Accepted in revised form: 19 January 1999

M. Bonnet · K.-D. Rogausch
J. Petermann (✉)
Department of Chemical Engineering
Institute of Material Science
University of Dortmund
Emil-Figge-Strasse 66
D-44221 Dortmund, Germany

Abstract The appearance of an endothermic annealing peak in semicrystalline poly(phenylene sulphide) and semicrystalline poly(ethylene terephthalate) after annealing at or above the cold-crystallization temperature is investigated by temperature-modulated differential scanning calorimetry, thermomechanical analysis and dynamic-mechanical analysis. The results indicate relaxation processes in the interlamellar amorphous phase, which is in a strongly constrained state after cold crystallization. During the annealing treatments rearranging processes take place. These processes result in a separation of the amorphous phase into an interlamellar relaxed and a "pseudo-crystalline" phase.

Key words Poly(phenylene sulphide) – Poly(ethylene terephthalate) – Annealing – Thermal history – Crystallization

Introduction

In the past, numerous studies have been devoted to the correlation between thermal history, melting behaviour and morphology of poly(phenylene sulphide) (PPS) [1–7], poly(ethylene terephthalate) (PET) [8–14] and poly (ether etherketone) [15–24]. After crystallization from the glassy amorphous state (cold crystallization) and subsequent annealing treatment between the crystallization and the melting temperature, changes in the amorphous phase take place. In differential scanning calorimetric measurements, an endothermic peak is found about 20 °C above the annealing temperatures ("annealing peak"). Until now many different kinds of measurements have been performed to understand the structural changes which take place during the annealing treatments [differential scanning calorimetry (DSC), temperature-modulated DSC (TMDSC), dynamic-mechanical analysis (DMA), wide-angle X-ray scattering and small-angle X-ray scattering]. Five different models have been put forward to explain the annealing peak.

1. Different crystal morphologies [4–6, 18]. According to this model the dual melting endotherms found in DSC are due to the melting of two crystal populations of different morphologies. No reorganization from one population into the other is assumed.
2. Different populations of crystallite sizes [19, 20]. Primary crystallization forms larger crystalline lamellae compared to the lamellae formed during secondary crystallization. The secondary formed lamellae melt first at lower temperatures and give rise to the extra melting endotherm in the DSC scans.
3. More or less perfect crystals [1, 3]. A second, less perfect pseudo-crystalline phase is induced on annealing. This phase melts just above the annealing temperature at which it was formed.
4. Crystal perfecting by melting and recrystallization [9, 10, 12, 13, 15, 16, 21, 23–25]. The "annealing peak" phenomenon is related to morphological changes in the microstructure of the semicrystalline samples during the DSC scan. Melting of the initial crystal morphology happens, which is characteristic of the previous crystallization history of the sample. The "annealing peak" is then indicative of the onset of melting of these crystals. In the temperature interval between the annealing and the final melting peak, all the crystals experience a continuous melting and recrystallization process.

5. Three-phase model [14, 27, 28]. In this model, the crystalline/amorphous interface is considered to be a ''rigid amorphous'' phase and separates the lamellar crystals from the amorphous areas.

None of the models fit with all the experimental results. It is the purpose of this paper to present some new results from TMDSC, thermo-mechanical analysis (TMA) and DMA. It will be demonstrated, that the three-phase model consisting of one crystalline but two amorphous (''pseudo-crystalline'' and relaxed) phases explains our results best.

Experimental

Materials and sample preparation

Isotropic sheets of amorphous PET (Hostaphan, thickness 130 μm) and PPS (Litex-P, thickness 105 μm) were kindly supplied by Kalle-Hoechst (Germany) and PCD-Polymers (Austria), respectively.

All heat treatments were carried out in an oven.

Isothermal crystallization of these amorphous sheets was performed at T_c = 134 °C for 90 min for PET and at T_c = 129 °C for 45 min for PPS.

Subsequently, isothermal annealing (T_a) was performed on the semicrystalline samples at $T_m > T_a \geq T_c$, with T_a = 134 and 154 °C for PET, and T_a = 129, 155 and 180 °C for PPS. The annealing times ranged from 24 to 552 h.

Temperature-modulated differential scanning calorimetry

The device used was an MDSC 2910-system from TA Instruments coupled with a TA 2000 control system. All measurements were performed with a heating rate of 5 K/min having a period of 60 s and an amplitude of 0.796 K. The input of the three parameters are visualized in a simple mathematical description of the heat flow

$$\underbrace{\frac{dQ}{dT}}_{\text{total HF}} = \underbrace{\frac{dT}{dt}[C_p + f_F(t,T)]}_{\text{reversing HF}} + \underbrace{f_N(t,T)}_{\text{nonreversing HF}} \quad (1)$$

with

dQ/dT: heat flow
dT/dt: heating rate
t: time
C_p: heat capacity
$f_R(t,T)$; $f_N(t,T)$: functions of time and temperature (kinetic answer)

Equation (1) implies, that the total heat flow is composed of a heat-capacity-proportional reversing part and a nonreversing part resulting from kinetic effects. The overall heat flow can be used to analyse complex events such as melting/recrystallization processes.

The heat capacity calibrations were performed with sapphire as a standard. Nitrogen was used for all measurements in order to avoid oxidation. The weights of the samples were 4.6 mg for PET and 3.5 mg for PPS.

Dynamic-mechanical analysis

A dynamic-mechanical analyser 2980 system from TA Instruments was used. All measurements were performed in a multifrequency mode with frequencies of 1, 2, 4, 8 and 16 Hz. The sample dimensions were 7 mm in length and 5 mm in width. An amplitude of 20 μm was chosen in order to guarantee a deformation within the linear response regime.

Thermo-mechanical analysis

The thermo-mechanical analyser 2940 system from TA Instruments coupled with a TA Thermal Analyst 2000 control system was used for the TMA measurements. TMA measures changes in the dimensions of a sample as a function of time, temperature and force (in our case as a function of temperature and a weak constant force). A ''thermal expansion coefficient'' (α) of the samples was calculated from the temperature-dependent dimensional change using the expansion as well as the film/fibre mode. The expansion is measured under compressional stresses and primarily designed to determine the thermal expansion coefficient and the glass-transition temperature. The film/fibre mode is a tension mode. It is used for investigating thermal histories of films and fibres.

For the film/fibre mode the samples were 2.54 mm in width and 17.5 mm in length and the thickness was as supplied (PET: 130 μm, PPS: 105 μm). All measurements were performed with heating rates of 3 K/min.

Results

Temperature-modulated differential scanning calorimetry

Crystallinity

The samples were annealed at the crystallization temperatures (T_c) till no measurable increase in crystallinity (χ) occurred (0.41 for PET and 0.38 for PPS after 90 min, respectively). Subsequently, the annealing treatment, causing the annealing peak, was performed for different times and temperatures. The crystallinities (χ) were determined from the DSC measurements using the melting enthalpy ΔH_m:

$$\chi = \frac{\Delta H_m}{\Delta H_m^0} \quad , \quad (2)$$

where ΔH_m^0 is the specific melting enthalpy.

The values for ΔH_m^0 were taken from the literature: ΔH_m^0 (PET) = 119.8 J/g [8]; ΔH_m^0 (PPS) = 112 J/g [26]. The respective crystallinities of the PET and PPS samples are presented in Tables 1 and 2.

Table 1 The crystallinity of annealed poly(ethylene terephthalate) for different annealing temperatures

T_a (°C)	ΔH_m (J/g)	χ
134	48.9	0.41
154	51.0	0.42

Table 2 The crystallinity of annealed poly(phenylene sulphide) for different annealing temperatures

T_a (°C)	ΔH_m (J/g)	χ
129	35.0	0.31
154	34.3	0.31
180	30.7	0.27

Melting behaviour

In addition to the "normal" melting peak, all annealed samples exhibit a second weak endothermic peak. The position of this peak depends on the annealing temperature and annealing time. A typical TMDSC run for an annealed PET sample, indicating the "annealing peak", is shown in Fig. 1.

The endothermic "annealing peak" appears in the nonreversing heat flow. In the reversing heat flow, which is directly proportional to the heat capacity, a T_g-like step is observed with its reflection point close to the peak maximum.

Influence of the annealing times and temperatures

The influences of annealing times and temperatures on the shape and position of the "annealing peak" were analysed from the nonreversing part of the heat flow. The position of the peak depends on the annealing time and is at its maximum 35 K above the corresponding annealing temperature. In these limits, the peak temperature increases with increasing annealing time. There is no influence of the annealing time on the step width in the reversing heat flow. The annealing-time-dependent peak temperatures for PET annealed at T_a = 134 and 154 °C are shown in Fig. 2 and those for PPS annealed at T_a = 129, 155 and 180 °C are shown in Fig. 3.

Dynamic-mechanical measurements

Figure 4 shows the temperature dependence of the storage Young's modulus (E') for PPS nonannealed material as well as for material annealed at 129, 155 and 180 °C for 48 h. The Young's modulus shows three different levels. Below T_g the value for the annealed material is larger than for nonannealed material. Its value increases with increasing annealing temperature. Above T_g, the moduli decrease but follow the same trend that the higher T_a the higher the modulus. A "final" common modulus for annealed and nonannealed samples of about 200 MPa is reached at about 25 °C above T_a.

Besides the β relaxation of the glass transition, a second but much smaller peak can be detected in the loss tangent (Fig. 5). The temperature position again depends on T_a (≈25 °C above annealing). A time and frequency (between 1 and 16 Hz) dependence cannot be resolved from our plots.

Thermo-mechanical analysis

A schematic picture for the temperature-dependent coefficient of thermal expansion for annealed PPS under small pressure (expansion modus) and under small tensile stress (film/fibre modus) is shown in Fig. 6.

Measurements were performed with film/fibre as well as expansion modus in order to distinguish between

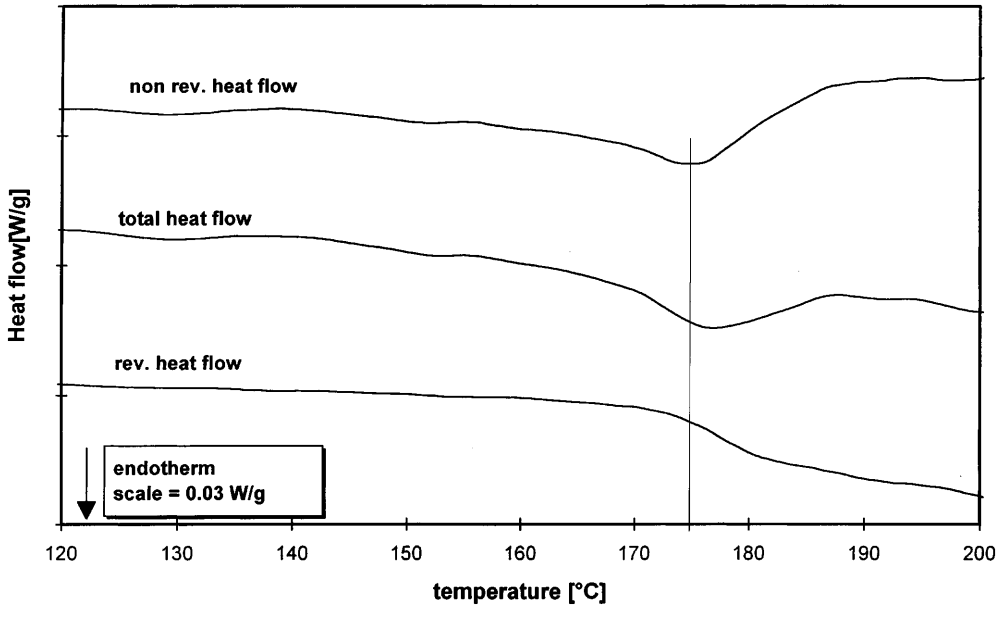

Fig. 1 Temperature-modulated differential scanning calorimetry scan for poly(ethylene terephthalate) (*PET*) annealed for 48 h at 154 °C

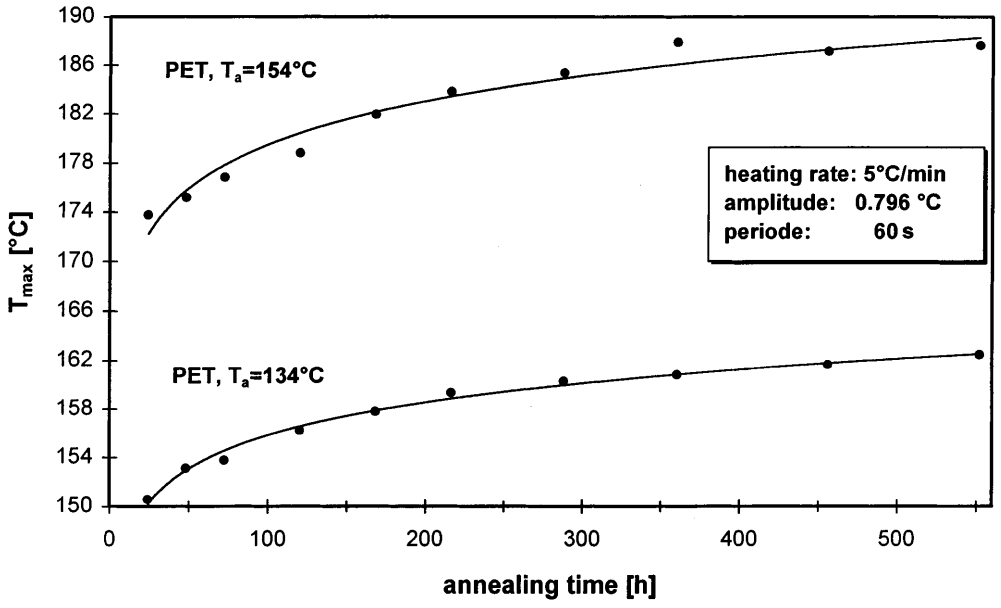

Fig. 2 "Annealing peak" maximum temperature T_{max} for PET versus the annealing times for two different annealing temperatures T_a

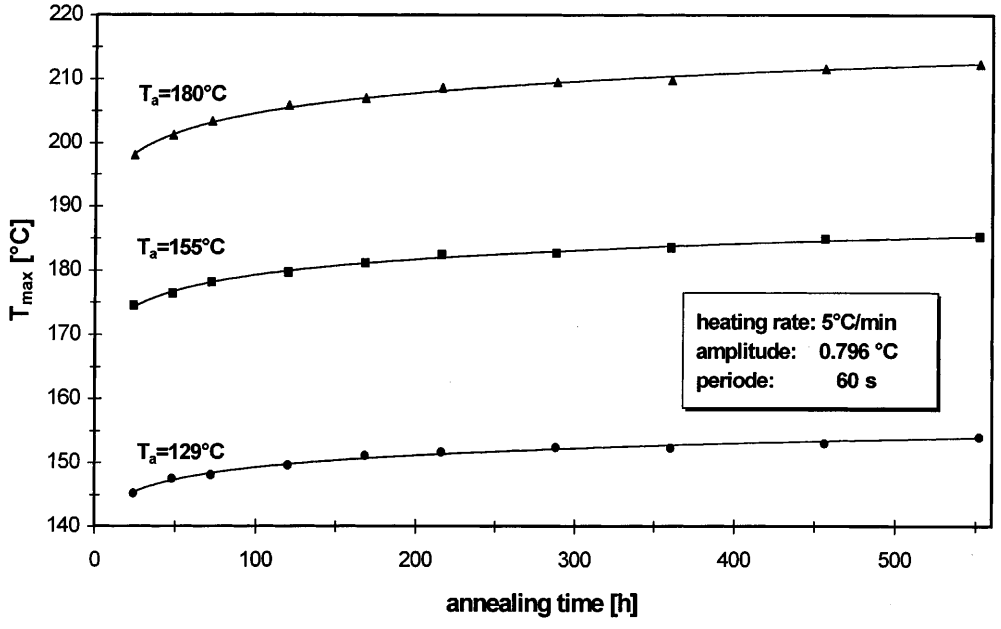

Fig. 3 "Annealing peak" maximum temperature T_{max} for poly(phenylene sulphide) (*PPS*) versus the annealing times for three different annealing temperatures

shrinking and softening. At the raised glass-transition temperature (105 °C) we observed a shrinking, while 10–30 K above T_a a softening can be observed.

Discussion

We will first correlate our results with the five models described earlier.

For the first three models (except the recrystallization model), the premelting phenomenon can be explained if we only consider the "normal" DSC scans. In TMDSC scans, the endothermic "annealing peak" takes place not in the reversing, but in the nonreversing heat flow. For the melting of a crystal population with a different morphology, or of lamellae with different thicknesses, or of less perfect crystals, the endothermic "annealing peak" should be found in the reversing heat flow as for the "normal" melting process. Especially, the explanation of the "annealing peak" by the melting of thinner lamellae is very doubtful, because the main argument of its supporters is a change in the long period, but in most works no significant change in the long period is reported [9].

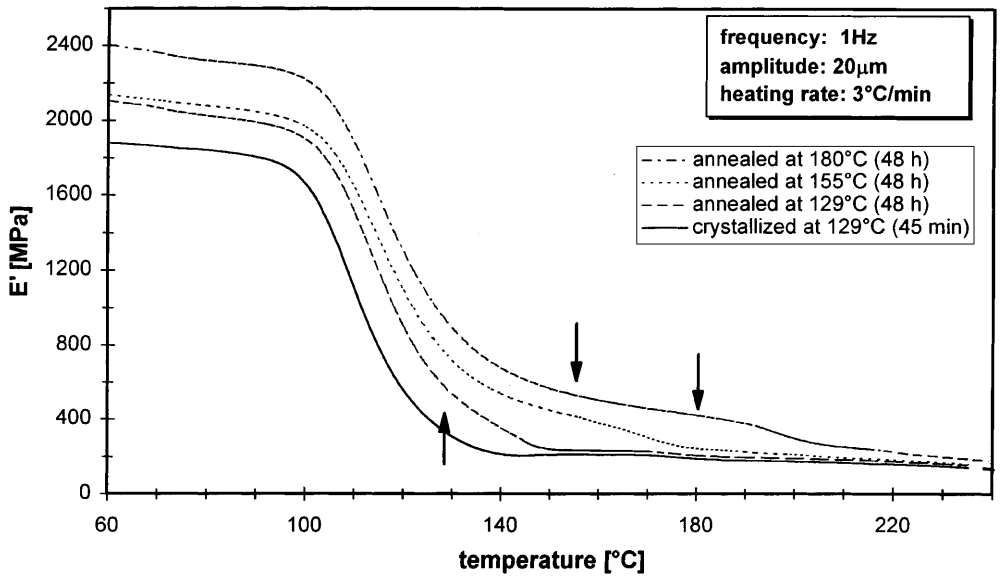

Fig. 4 Temperature dependence of the storage Young's modulus (E') for PPS. The *arrows* indicate the annealing temperature

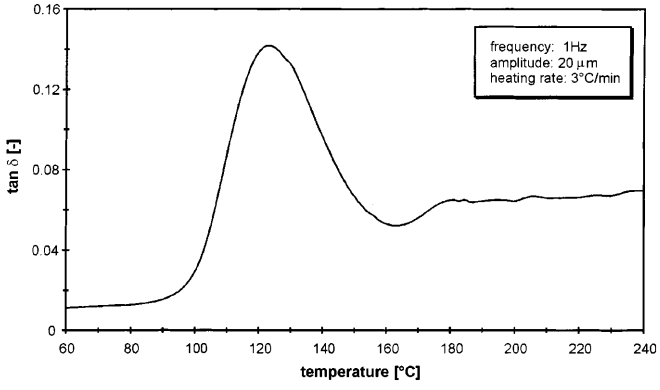

Fig. 5 Temperature-dependent loss tangent for PPS, annealed for 48 h at 155 °C

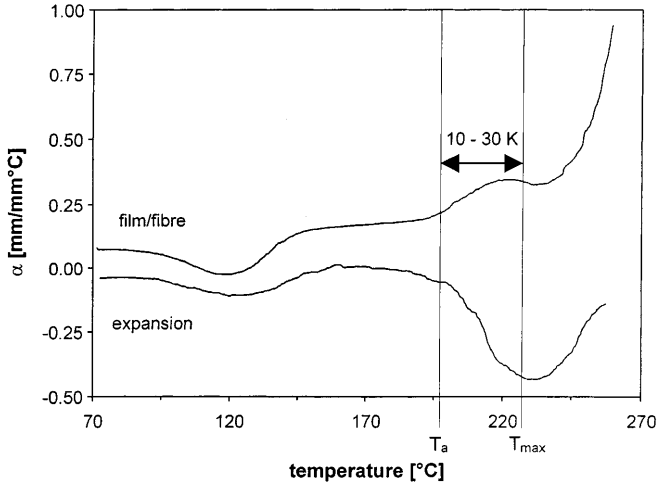

Fig. 6 Temperature-dependent coefficient of thermal expansion for annealed PPS (expansion and film/fibre modus)

Most of the papers that explain the "annealing peak" by melting and recrystallization processes that occur during heating above T_a, do not accept DSC as a suitable method to give direct information on the nature of the morphological changes involved. They argue, that melting and immediate recrystallization cannot be detected by DSC; however, TMDSC is well known as a sensitive method to investigate melting and recrystallization processes separately [29] and also solid-state transformation processes can be detected [30, 31]. For a simultaneous melting and recrystallization process, an endothermic peak in the reversing heat flow and an exothermic peak in the nonreversing heat flow is expected. Instead, we observe an endothermic peak in the nonreversing heat flow and a transition step in the reversing heat flow. Also the softening of the annealed materials in the "annealing peak", investigated by DMA (see also Refs. [1, 3]) and TMA, cannot be explained by recrystallization.

Our experimental results imply that cold crystallization is a process which is still far away from thermal equilibrium and is mainly controlled by the rate of crystal formation. The nonequilibrium state can manifest itself in an imperfection of the crystal, in a strongly constrained amorphous state or in both. Annealing at elevated temperatures will eventually bring the system to a minimum free-energy state (perfect crystals and/or relaxed amorphous material). From all our experiments we conclude, that a three-phase model may fit our results very well, but being slightly different from that of Cheng et al. [14] and Schick and coworkers [27, 28]. After cold crystallization from the glassy phase at 134 °C for 90 min, the amorphous phase is under constraint conditions (Fig. 7a). The glass-transition step at 80 °C for completely amorphous PET is shifted to

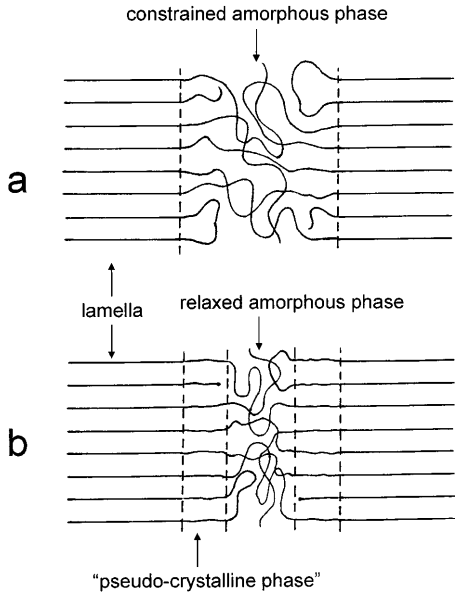

Fig. 7 The crystal/amorphous interphase **a** after crystallization at T_c from the glassy state and **b** after annealing at T_a with $T_c < T < T_m$

105 °C, belonging to the constraint amorphous phase. During annealing at $T_c < T_a < T_m$, the constraint amorphous phase tries to reduce strain energy at the crystal interface and separates into two amorphous phases: one highly ordered "pseudo-crystalline" phase (at the interface) and a relaxed amorphous phase (Fig. 7b). The "annealing peak" results from the relaxation of the "pseudo-crystalline" phase. An increase in Young's modulus for the annealed material is the consequence. In the TMDSC scan, this structure exhibits an irreversible endothermic process in the nonreversing heat flow just above T_a, when transforming the "pseudo-crystalline" structure into the relaxed amorphous phase, and a simultaneous transition step in the reversing heat flow, due to an increase in the heat capacity. Also, the softening (decreasing of the Young's modulus) observed in the TMA and DMA measurement is consistent with our model. Similar considerations have recently been presented by Hauser et al. [32], but in their model all the imperfections which bring the system out of equilibrium are supposed in the crystalline state. Direct visualizations of the morphologies by transmission electron microscopy or atomic force microscopy may help to distinguish between the two morphological models.

Conclusion

The "annealing peak" of cold crystallized PET and PPS is explained by a "three-phase" model: crystalline, "pseudo-crystalline" amorphous, and relaxed amorphous phase, which are formed during annealing. The "annealing peak", observed in conventional DSC scans, is explained by a relaxation of the "pseudo-crystalline" phase into the relaxed amorphous component. Our TMDSC, DMA and TMA measurements are consistent with this model.

Acknowledgements The financial support of the Deutsche Forschungsgemeinschaft is gratefully acknowledged. The authors also want to thank G. Strobl for very stimulating discussions.

References

1. Breach CD, Hu X (1996) J Mater Sci Lett 15:1416
2. Jimbo T, Asai S, Sumita M (1997) J Macromol Sci Phys B 36:381
3. Scobbo JJ, Hwang CR (1994) Polym Eng Sci 34:1744
4. Chung JS, Cebe P (1992) Polymer 33:2312
5. Chung JS, Cebe P (1992) Polymer 33:2325
6. Chung JS, Cebe P (1990) Polym Comput 11:265
7. Deporter J, Baird DG (1993) Polym Comput 14:201
8. Toda T, Yoshida H, Fukunishi K (1997) Polymer 38:5463
9. Fontaine F, Ledent J, Groenickx G, Reynaers H (1982) Polymer 23:185
10. Jonas AM, Russell TP, Yoon DY (1994) Colloid Polym Sci 272:1344
11. Bove L, D'Aniello C, Gorrasi G, Guardagno L, Vittoria V (1997) Polym Bull 38:579
12. Holdsworth PJ, Turner-Jones A (1971) Polymer 12:195
13. Groenickx G, Reynears H (1980) J Polym Sci Polym Phys Ed 18:1325
14. Cheng SZD, Cao MY, Wunderlich B (1986) Macromolecules 19:1868
15. Fougnies C, Camman P, Disière M, Koch MHJ (1997) Macromolecules 30:1392
16. Blundell DJ (1987) Polymer 28:2248
17. Blundell DJ, Osborn BN (1983) Polymer 24:953
18. Bassett DC, Olley RH, Raheil IAM (1988) Polymer 29:1745
19. Verma R, Marand H, Hsiao B (1996) Macromolecules 29:7767
20. Hsiao BS, Gardner KH, Wu DQ, Chu B (1993) Polymer 34:3986
21. Jonas AM, Russell TP, Yoon DY (1995) Macromolecules 28:8491
22. Cebe P, Hong S-D (1986) Polymer 27:1183
23. Lee Y, Porter RS (1987) Macromolecules 20:1336
24. Lee Y, Porter RS, Lin JS (1989) Macromolecules 22:1754
25. Ikeda M (1968) Chem Abstr 69:19666
26. Huo P, Cebe P (1992) Colloid Polym Sci 270:840
27. Schick C, Merzlyakov M, Wunderlich B (1998) Polym Bulletin 40:297
28. Alsleben M, Schick C (1994) Thermochim Acta 238:203
29. Gill PS, Sauerbrunn SR, Reading M (1993) J Therm Anal 40:931
30. Loos J, Hückert A, Petermann J (1996) Colloid Polym Sci 274:1006
31. Karger-Kocsis J, Shang PP (1998) J Therm Anal 51:237
32. Hauser G, Schmitdke J, Strobl G (1998) Macromolecules 31:6250